## Note after first publication

This version of the Electronic Supplementary Information replaces the version first published on 28th September 2022, which contained errors in the CCDC numbers listed for the compounds reported. The correct CCDC numbers are 2321694–2321699.

# Post-synthetic molecular modifications based on Schiff base condensations for designing functional paddlewheel diruthenium(II, II) complexes

Chisa Itoh,[a] Haruka Yoshino,[a,b] Taku Kitayama,[a] Wataru Kosaka,[a,b] and Hitoshi Miyasaka*[a,b]

[a] *Department of Chemistry, Graduate School of Science, Tohoku University, 6-3 Arama-ki-Aza-Aoba, Aoba-ku, Sendai 980-8578, Japan*

[b] *Institute for Materials Research, Tohoku University, 2-1-1 Katahira, Aoba-ku, Sendai 980-8577, Japan*

*Corresponding author:
Prof. Dr. Hitoshi Miyasaka
Institute for Materials Research
Tohoku University
2–1–1 Katahira, Aoba-ku, Sendai, 980-8577, Japan
E-mail: miyasaka@imr.tohoku.ac.jp
Tel: +81-22-215-2030
FAX: +81-22-215-2031

**Contents for SI**

## Experimental Section

### Materials

All synthesis procedures were performed under anaerobic conditions using standard Schlenk-line techniques in a commercial glovebox under nitrogen atmosphere. All chemicals were purchased from commercial sources and were of reagent grade. The solvents were dried using common drying agents and distilled under $N_2$ prior to use. The precursor complex $[Ru_2(CH_3CO_2)_4Cl]$ was prepared according to a previously reported procedure.[1] Some compounds have interstitial THF molecules as crystallization solvents, all or part of which were eliminated when the crystal sample was evacuated, and water molecules were sometimes replaced or included in samples, as realized from elemental analysis.

### Synthesis of $[Ru_2\{p\text{-}(CHO)ArCO_2\}_4(THF)_2]\cdot 2THF$ (*p*-CHO)

Single crystals of $[Ru_2^{II,II}\{p\text{-}(CHO)ArCO_2\}_4(THF)_2]\cdot 2THF$ (***p*-CHO**) were synthesized in a stepwise manner via a ligand substitution process involving $[Ru_2^{II,III}]^+$, followed by reduction to the corresponding $[Ru_2^{II,II}]$ products.[2] $[Ru_2^{II,III}(CH_3CO_2)_4Cl]$ (710 mg, 1.5 mmol) and *p*-formylbenzoic acid (909 mg, 6.05 mmol) were refluxed in a 1:1 solution of MeOH and $H_2O$ (40 mL) at 105 ℃ for 12 h under aerobic conditions to synthesize $[Ru_2^{II,III}\{p\text{-}(CHO)ArCO_2\}_4Cl]$. The obtained red precipitate was collected by filtration, washed with water, and dried *in vacuo*. Without further purification, a THF solution (40 mL) of the crude product and Zn powder (130 mg, 2 mmol) were stirred for 4 d under a nitrogen atmosphere. The reddish-colored solution was filtered, and the filtrate was layered with *n*-hexane and allowed to stand for at least one week to afford ***p*-CHO** as brown crystals. The crystal sample was then dried under vacuum for elemental analysis. Yield: 68%. Elemental analysis (%) for $[Ru_2\{p\text{-}(CHO)ArCO_2\}_4(THF)_2]\cdot H_2O$, $C_{40}H_{38}O_{15}Ru_2$, calc.: C, 50.00; H, 3.99; Found: C, 50.06; H, 3.92. IR (KBr): $\nu(CO_2)$ = 1591, 1403 $cm^{-1}$.

### Synthesis of $[Ru_2\{p\text{-}(CHO)ArCO_2\}_2\{2,6\text{-}(CF_3)_2ArCO_2\}_4(THF)_2]$ (Hete-*p*-CHO)

$[Ru_2^{II,III}\{p\text{-}(CHO)ArCO_2\}_4Cl]$ (834 mg, 1 mmol) and 2,6-bis(trifluoromethyl)benzoic acid (2 mmol, 516 mg) were refluxed in a 1:3 solution of MeOH and $H_2O$ (40 mL) at 120 ℃ for 12 h under aerobic conditions to obtain $[Ru_2\{p\text{-}(CHO)ArCO_2\}_2\{2,6\text{-}(CF_3)_2ArCO_2\}_2Cl]$. A THF solution (40 mL) of $[Ru_2\{p\text{-}(CHO)ArCO_2\}_2\{2,6\text{-}(CF_3)_2ArCO_2\}_2Cl]$ (950 mg, 0.9 mmol) and Zn powder (117 mg, 1.8 mmol) were stirred for 4 d under a nitrogen atmosphere. The brown solution was filtered, and the filtrate was layered with *n*-hexane and allowed to stand for at least one week to afford **Hete-*p*-CHO** as brown crystals. The crystal sample was then dried under vacuum for elemental analysis. Yield: 65%. Elemental analysis (%) for $[Ru_2\{p\text{-}(CHO)ArCO_2\}_2\{2,6\text{-}(CF_3)_2ArCO_2\}_4(THF)_2]\cdot 2H_2O$, $C_{42}H_{36}O_{14}F_{12}Ru_2$, calc.: C, 44.23; H, 3.04; Found: C, 44.43; H, 3.08. IR (KBr): $\nu(CO_2)$ = 1591, 1403 $cm^{-1}$.

**Syntheses of imine-linked $[Ru_2]$ Complexes, $[Ru_2(Ph\text{-}NC\text{-}ArCO_2)_4(THF)_2]$ (1), $[Ru_2\{Ar(OMe)\text{-}NC\text{-}ArCO_2\}_4(THF)_2]\cdot THF$ (2), $[Ru_2\{Ar(OMe)\text{-}NC\text{-}ArCO_2\}_2\{2,6\text{-}(CF_3)_2ArCO_2\}_2(THF)_2]\cdot THF$ (3), $[Ru_2(Pyrene\text{-}NC\text{-}ArCO_2)_2\{2,6\text{-}(CF_3)_2ArCO_2\}_2(THF)_2]\cdot 2THF$ (4)**

Single crystals of imine-linked paddlewheel-type diruthenium(II, II) complexes were prepared using a post-synthetic molecular modification method *via* imine formation through the reaction of ***p*-CHO** or **Hete-*p*-CHO** with monoamines. The detailed synthesis procedure for $[Ru_2(Ph\text{-}NC\text{-}ArCO_2)_4(THF)_2]$ (**1**) is described. Aniline (0.8 mmol, 74 μL) was added to a dehydrated THF solution (20 mL) of ***p*-CHO** (188 mg, 0.2 mmol) and stirred for one day under a nitrogen atmosphere. The brown solution was filtered, and the filtrate was layered with *n*-hexane and allowed to stand for at least two weeks to afford **1** as brown crystals. The crystal sample was then dried under vacuum for elemental analysis. Yield: 67%. Elemental analysis (%) for $[Ru_2(Ph\text{-}NC\text{-}ArCO_2)_4(THF)]\cdot 3.5H_2O$, $C_{64}H_{63}O_{12.5}N_4Ru_2$, calc.: C, 58.39; H, 4.49; N, 4.54; Fou{nd: C, 58.22; H, 4.22; N, 4.40. IR (KBr): $\nu(CO_2)$ = 1579, 1403 $cm^{-1}$.

$[Ru_2\{Ar(OMe)\text{-}NC\text{-}ArCO_2\}_4(THF)_2]\cdot THF$ (**2**) was synthesized as brown crystals in a similar manner to that used for **1**, except for the use of *p*-Anisidine (0.8 mmol, 99 mg). The crystal sample

was then dried under vacuum for elemental analysis. Yield: 50%. Elemental analysis (%) for $[Ru_2\{Ar(OMe)\text{-}NC\text{-}ArCO_2\}_4(THF)_2]\cdot 1.5H_2O$, $C_{68}H_{67}O_{15.5}N_4Ru_2$, calc.: C, 58.74; H, 4.86; N, 4.03; Found: C, 58.66; H, 4.96; N, 3.78. IR (KBr): $\nu(CO_2)$ = 1585, 1404 $cm^{-1}$.

$[Ru_2\{Ar(OMe)\text{-}NC\text{-}ArCO_2\}_2\{2,6\text{-}(CF_3)_2ArCO_2\}_2(THF)_2]\cdot THF$ (**3**) was synthesized as brown crystals in a similar manner to that used for **2**, except for the use of **Hete-*p*-CHO** (0.15 mmol, 153 mg). The crystal sample was then dried under vacuum for elemental analysis. Yield: 68%. Elemental analysis (%) for $[Ru_2\{Ar(OMe)\text{-}NC\text{-}ArCO_2\}_2\{2,6\text{-}(CF_3)_2ArCO_2\}_2(THF)_2]$, $C_{56}H_{46}O_{12}F_{12}N_2Ru_2$, calc.: C, 49.13; H, 3.39; N, 2.05; Found: C, 49.17; H, 3.49; N, 2.33. IR (KBr): $\nu(CO_2)$ = 1586, 1406 $cm^{-1}$.

$[Ru_2(Pyrene\text{-}NC\text{-}ArCO_2)_2\{2,6\text{-}(CF_3)_2ArCO_2\}_2(THF)_2]\cdot 2THF$ (**4**) was synthesized as brown crystals in a similar manner to that used for **3**, except for the use of 1-aminopyrene (0.3 mmol, 65 mg). The crystal sample was then dried under vacuum for elemental analysis. Yield: 62%. Elemental analysis (%) for $[Ru_2(Pyrene\text{-}NC\text{-}ArCO_2)_2\{2,6\text{-}(CF_3)_2ArCO_2\}_2(THF)_2]\cdot 1.5(THF)$, $C_{80}H_{62}O_{11.5}F_{12}N_2Ru_2$, calc.: C, 57.69; H, 3.75; N, 1.68; Found: C, 57.97; H, 3.55; N, 1.96. IR (KBr): $\nu(CO_2)$ = 1581, 1400 $cm^{-1}$.

**Physical Measurements**

Elemental analyses of carbon, hydrogen, and nitrogen were performed at the Division of the Graduate School of Science, Tohoku University. Infrared (IR) spectra were recorded on a JASCO FT/IR-4200 spectrophotometer with KBr disks in the range of 650–4000 $cm^{-1}$ at room temperature. The magnetic properties were investigated using a Quantum Design MPMS-XL SQUID in the range of 1.8–300 K with a magnetic field of 0.1 T. The diamagnetic correction was calculated using Pascal's constant.[3] Cyclic voltammograms (CVs) were recorded in THF with tetra-n-butylammonium hexafluorophosphate ($n$-$Bu_4N(PF_6)$, 0.1 M) as the supporting electrolyte under nitrogen atmosphere using an electrochemical analyzer (ALS/[H] CH Instruments Model 600A) with a glassy carbon electrode as the working electrode, a Pt counter electrode, and a $Ag/AgNO_3$ reference electrode. First,

the CV of a solvent containing only the supporting electrolyte was measured. The desired compounds were then added to this solution ([compound] = $1 \times 10^{-3}$ M), and the CVs were acquired at a scan rate of 0.05 V $s^{-1}$. Finally, the CV potentials in THF were adjusted using a ferrocene/ferrocenium couple ($Fc/Fc^+$ = 213 mV ($\Delta E$ = 91 mV) vs. $Ag/Ag^+$) as an internal standard.

**Single-crystal X-ray diffraction**

Single-crystal X-ray data were recorded on a Rigaku XtaLAB SynergyCustom diffractometer with monochromated Mo-Kα radiation ($\lambda$ = 0.71073 Å) equipped with a Hybrid Pixel Array Detector. A single crystal was mounted on a polymer film with liquid paraffin, and the temperature was controlled by a nitrogen flow using a Rigaku $GN_2$ apparatus. Data integration and reduction were performed using CrysAlisPro software.[4] The structures were solved with the SHELXT structure solution program using direct methods and refined with the SHELXL refinement package using least squares minimization with the Olex2 crystallography software.[5,6] Hydrogen atoms were included in idealized positions and refined using a riding model. Relevant crystal data collection and refinement of the crystal structure of **1** are summarized in **Table S1**. CCDC 2321694–2321699

**Computational analysis**

Theoretical *ab initio* calculations were performed using DFT formalism, as implemented in the Gaussian 09 software,[7] employing Beck's three-parameter hybrid functional with the correlation functional of Lee, Yang, and Parr (B3LYP).[8] Unrestricted open-shell calculations were performed for molecules containing [$Ru_2$] units. The effective core potential basis function LanL2TZ with polarization (LanL2TZ(f))[9,10,11] for Ru atoms and the 6-31G basis sets with polarization and diffusion functions (6-31+G(d))[12,13,14,15,16] for C, H, F, and O atoms were adopted. Spin polarization with $S_Z$ = 1 (triplet spin multiplicity) was used for the [$Ru_2$] units in the calculations. Atomic coordinates determined by X-ray crystallography were used in the calculations.

**Table S1.** Crystallographic data and refinement parameters.

| Compound | ***p*-CHO** | **Hete-*p*-CHO** | **1** | **2** | **3** | **4** |
|---|---|---|---|---|---|---|
| CCDC | 2321694 | 2321695 | 2321696 | 2321697 | 2321698 | 2321299 |
| Formula | $C_{48}H_{52}O_{16}Ru_2$ | $C_{42}H_{32}F_{12}O_{12}Ru_2$ | $C_{64}H_{56}N_4O_{10}Ru_2$ | $C_{72}H_{58}N_4O_{15}Ru_2$ | $C_{60}H_{42}F_{12}N_2O_{13}Ru_2$ | $C_{82}H_{64}F_{12}N_2O_{12}Ru_2$ |
| $T$ / K | 102 | 102 | 102 | 102 | 102 | 102 |
| Formula weight | 1087.03 | 1158.81 | 1243.26 | 1421.36 | 1429.09 | 1699.49 |
| Crystal system | Triclinic | Triclinic | Monoclinic | Tetragonal | Triclinic | Triclinic |
| Space group | $P\bar{1}$ | $P\bar{1}$ | $P2_1/c$ | $P4_2/m$ | $P\bar{1}$ | $P\bar{1}$ |
| $a$ / Å | 10.1030(3) | 9.2598(5) | 18.5812(8) | 17.6693(7) | 9.8839(5) | 10.2340(2) |
| $b$ / Å | 11.3908(4) | 10.9329(8) | 16.5825(6) | 17.6693(7) | 11.1000(7) | 12.2457(3) |
| $c$ / Å | 11.9634(5) | 11.6726(8) | 8.7476(3) | 32.9554(14) | 14.5687(7) | 16.2701(3) |
| $\alpha$ / ° | 63.205(4) | 63.049(7) | 90 | 90 | 71.855(5) | 111.777(2) |
| $\beta$ / ° | 71.840(3) | 86.323(5) | 91.443(4) | 90 | 71.325(4) | 103.696(2) |
| $\gamma$ / ° | 71.697(3) | 84.182(5) | 90 | 90 | 86.942(5) | 93.940(2) |
| $V$ / Å$^3$ | 1143.02(8) | 1047.71(14) | 2694.48(18) | 10288.8(9) | 1436.99(15) | 1811.75(7) |
| $Z$ | 1 | 1 | 2 | 6 | 1 | 1 |
| $R_1$[a] | 0.0249 | 0.0369 | 0.0430 | 0.0885 | 0.0580 | 0.0528 |
| $wR_2$[b] | 0.0635 | 0.0902 | 0.1082 | 0.2576 | 0.1420 | 0.1502 |
| Goodness of Fit | 1.067 | 1.034 | 1.041 | 1.049 | 1.021 | 1.082 |

[a] $R_1 = R = \Sigma||F_o|-|F_c||/\Sigma|F_o|$. [b] $wR_2 = [\Sigma w(F_o^2-F_c^2)^2/\Sigma w(F_o^2)^2]^{1/2}$.

**Table S2.** Relevant bond lengths (Å) around the Ru centers. The bond lengths of **2** are the average of Unit A and Unit B.

| Compound | Ru-Ru/Å | Averaged Ru-$O_{eq}$/Å | Ru-$O_{ax}$/Å |
|---|---|---|---|
| ***p*-CHO** | 2.2689(3) | 2.0636 | 2.3578(12) |
| **Hete-*p*-CHO** | 2.2663(4) | 2.0633 | 2.3282(18) |
| **1** | 2.2688(4) | 2.066 | 2.355(2) |
| **2** | 2.260 (ave.) | 2.061 | 2.307 (ave.) |
| **3** | 2.2695(5) | 2.064 | 2.326(2) |
| **4** | 2.2769(4) | 2.063 | 2.355(2) |

**Table S3.** Magnetic parameters of ***p*-CHO**, **Hete-*p*-CHO**, **1**, **2**, **3**, and **4** obtained from the best-fit of $\chi$ vs. $T$ data using a Curie equation for $S = 1$ with $g = 2.00$ (fix) and $zJ' = 0$ (fix).

| Compound | $D$ [K] | $\chi_{TIP}$ [$\times 10^{-6}$ cm$^3$ mol$^{-1}$] | $\rho$ [$\times 10^{-3}$] |
|---|---|---|---|
| ***p*-CHO** | 360.8(13) | 114(9) | 46.6(3) |
| **Hete-*p*-CHO** | 375.8(14) | 109(9) | 46.2(2) |
| **1** | 400(3) | 100(16) | 59.1(7) |
| **2** | 382(3) | 109(16) | 65.3(7) |
| **3** | 377(3) | 77(28) | 6.72(5) |
| **4** | 358.9(16) | 127(11) | 24.7(4) |

**Table S4.** Estimated energy levels (eV) of π*- and δ*-characteristic orbitals of ***p*-CHO**, **Hete-*p*-CHO**, **1**, **2**, **3**, and **4** obtained by DFT calculation. These energy levels of **2** are the average of Unit A and Unit B.

| Electron character | Orbital character | ***p*-CHO** | **Hete-*p*-CHO** | **1** | **2** | **3** | **4** |
|---|---|---|---|---|---|---|---|
| $\beta$ | $\pi^*$ | –2.52250 | –2.20766 | –2.02099 | –1.81201 | –1.85119 | –2.20303 |
| | $\pi^*$ | –2.55325 | –2.28957 | –2.11079 | –1.87541 | –1.93881 | –2.25583 |
| | $\delta^*$ | –4.84118 | –4.68199 | –4.43410 | –4.14158 | –4.30267 | –4.51573 |
| $\alpha$ | $\delta^*$ | –5.27003 | –5.10758 | –4.86077 | –4.56934 | –4.72716 | –4.93887 |
| | $\pi^*$ | –5.47194 | –5.31357 | –5.06785 | –4.77941 | –4.94975 | –5.16119 |
| | $\pi^*$ | –5.58786 | –5.39194 | –5.17942 | –4.88907 | –5.01343 | –5.24908 |

**Table S5.** Electrochemical data of ***p*-CHO**, **Hete-*p*-CHO**, **1**, **2**, **3**, and **4** measured in THF containing 0.1 M *n*-$Bu_4N(PF_6)$ under $N_2$ (mV vs. $Ag/Ag^+$)[a] and the HOMO level calculated by density functional theory

| Compound | $E_a$/mV | $E_c$/mV | $E_{1/2}$/mV | $\Delta E_p$/mV | HOMO energy/eV | p$K_a$ of benzoate[b] | $\Sigma(x\sigma_m + y\sigma_p)$[e] | $\Sigma(x\sigma_m + y\sigma_p + z\sigma_o)$[e] |
|---|---|---|---|---|---|---|---|---|
| ***p*-CHO** | 127 | 7 | 67 | 120 | –4.8412 | 3.78 [d] | 0.42 | 0.42 |
| **Hete-*p*-CHO** | 301 | 68 | 185 | 233 | –4.6820 | 2.27[c]/3.78[d] | 0.42 | 0.42 |
| **1** | 59 | –69 | –5 | 128 | –4.4341 | 4.257 [d] | – | – |
| **2** | –14.5 | –139.5 | –78 | 125 | –4.1416 | 4.256 [d] | – | – |
| **3** | 243.5 | –144.5 | 50 | 388 | –4.3027 | 2.27 [c] /4.256 [d] | – | – |
| **4** | 223 | 41 | 133 | 182 | –4.5157 | 2.27 [c] /4.263 [d] | – | – |

[a] The ferrocene/ferrocenium couple, $Fc/Fc^+$ = 213 mV, was observed under the same conditions described in the Experimental section of the text. [b] Predicted values calculated using Advanced Chemistry Development (ACD/Labs) Software V11.02, which were obtained from SciFinder-*n* data-base. [c] p$K_a$ of 2,6-$CF_3ArCO_2H$. [d] p$K_a$ of *p*-(CHO)$ArCO_2H$ and imine-linked benzoic acid.

**Table S6.** Electrochemical data of ***p*-CHO**, **Hete-*p*-CHO**, **1**, **2**, **3**, and **4** measured in THF containing 0.1 M *n*-$Bu_4N(PF_6)$ under $N_2$ (mV vs. $Fc/Fc^+$)[a] and the HOMO level calculated by density functional theory

| Compound | $E_a$/mV | $E_c$/mV | $E_{1/2}$/mV | $\Delta E_p$/mV | HOMO energy/eV | p$K_a$ of benzoate[b] | $\Sigma(x\sigma_m + y\sigma_p)$[e] | $\Sigma(x\sigma_m + y\sigma_p + z\sigma_o)$[e] |
|---|---|---|---|---|---|---|---|---|
| ***p*-CHO** | –86 | –206 | –146 | 120 | –4.8412 | 3.78 [d] | 0.42 | 0.42 |
| **Hete-*p*-CHO** | 88 | –145 | –28 | 233 | –4.6820 | 2.27[c]/3.78[d] | 0.42 | 0.42 |
| **1** | –154 | –282 | –218 | 128 | –4.4341 | 4.257 [d] | – | – |
| **2** | –227.5 | –352.5 | –291 | 125 | –4.1416 | 4.256 [d] | – | – |
| **3** | 30.5 | –357.5 | –163 | 388 | –4.3027 | 2.27 [c] /4.256 [d] | – | – |
| **4** | 10 | –172 | –80 | 182 | –4.5157 | 2.27 [c] /4.263 [d] | – | – |

[a] The ferrocene/ferrocenium couple, $Fc/Fc^+$ = 213 mV, was observed under the same conditions described in the Experimental section of the text. [b] Predicted values calculated using Advanced Chemistry Development (ACD/Labs) Software V11.02, which were obtained from SciFinder-*n* data-base. [c] p$K_a$ of 2,6-$CF_3ArCO_2H$. [d] p$K_a$ of *p*-(CHO)$ArCO_2H$ and imine-linked benzoic acid.

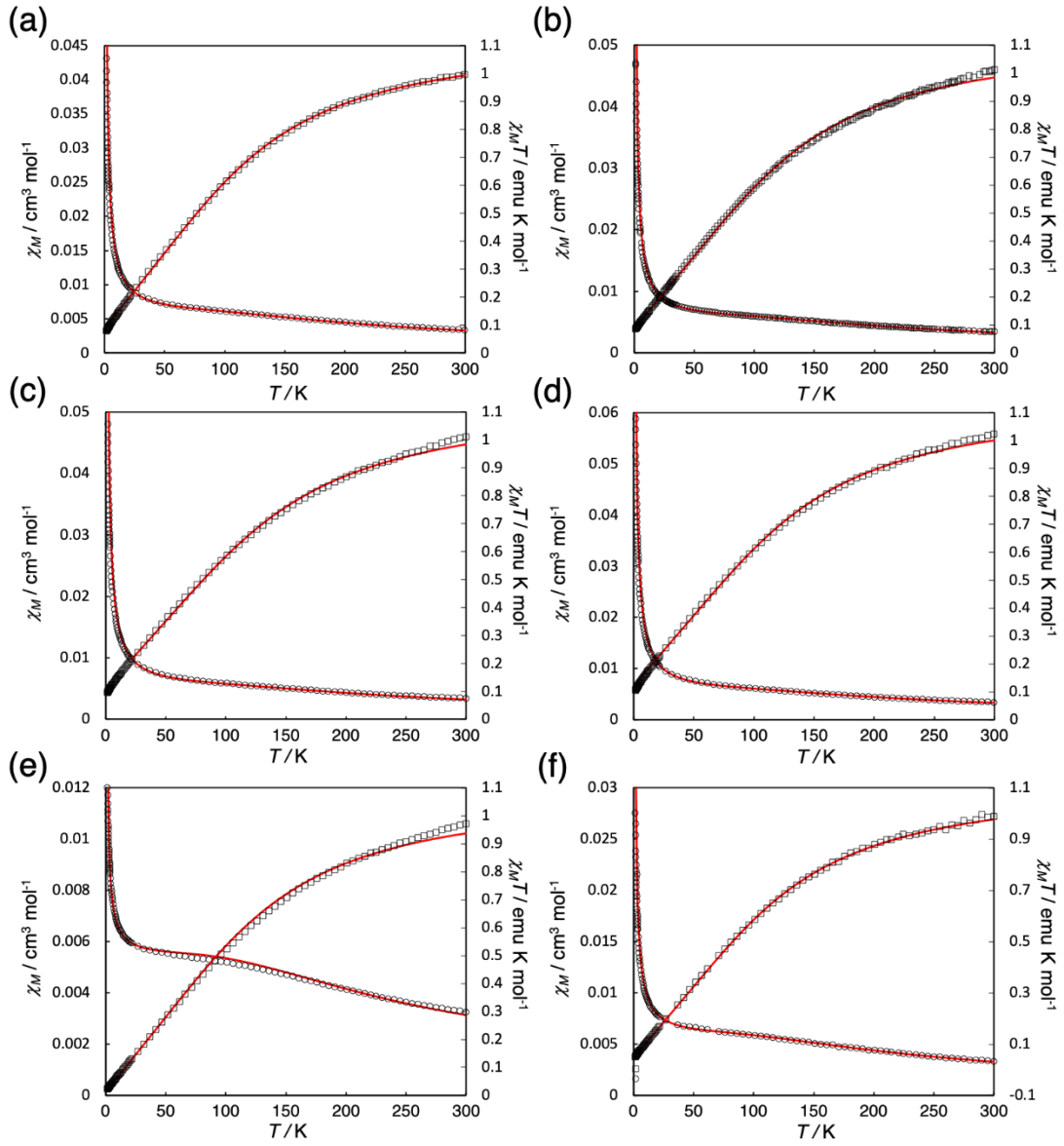


**Fig. S1**. Temperature dependence of $\chi$ (○) and $\chi T$ (□) of (a) ***p*-CHO**, (b) **Hete-*p*-CHO**, (c) **1**, (d) **2**, (e) **3**, and (f) **4**, where the red solid lines represent simulated curves based on a Curie paramagnetic model with $S = 1$ taking into account zero-field splitting ($D$), and impurity with $S = 3/2$ ($\rho$).

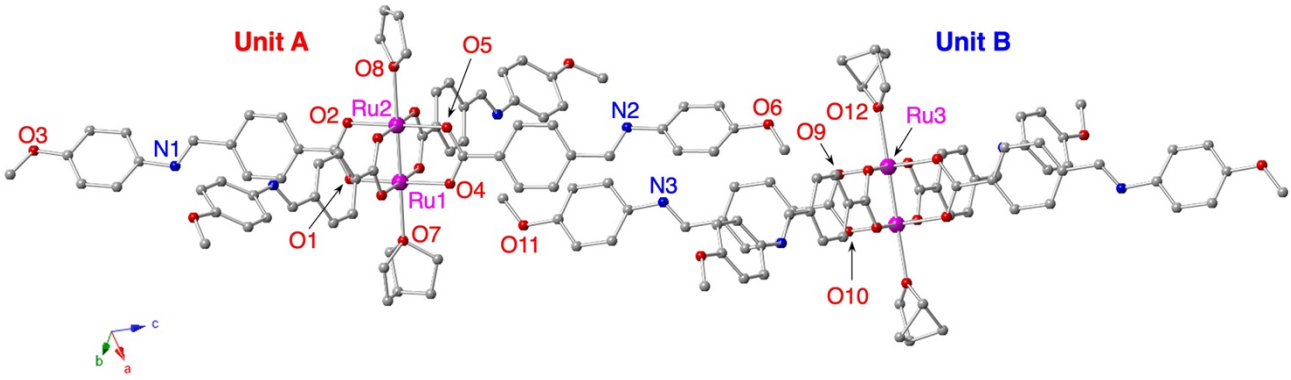


**Fig. S2**. Asymmetric molecular units A and B of **2** with numbering scheme for some unique atoms. Atomic code: Ru, pink; C, grey; N, blue; O, red; respectively. H atoms and crystallization solvents were omitted for clarity.

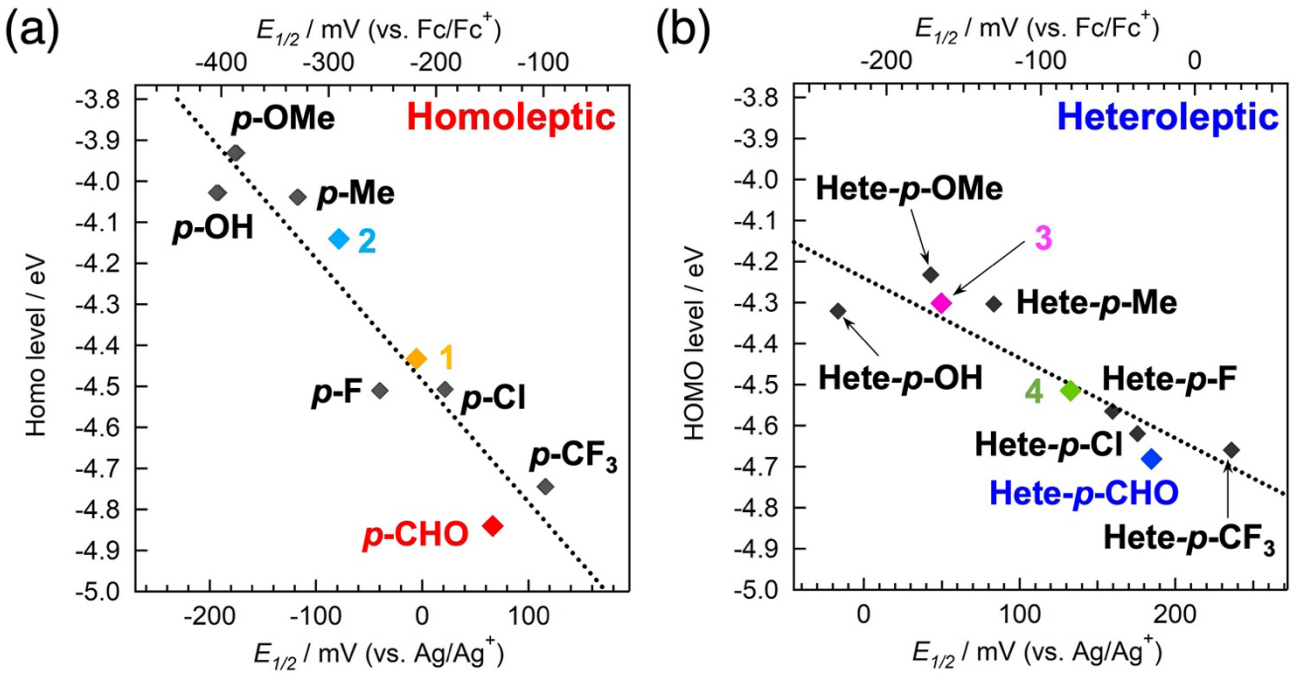


**Fig. S3.** (a, b) HOMO level vs $E_{1/2}$ plots (vs. Ag/Ag$^+$ and vs. Fc/Fc$^+$) for the corresponding benzoic acids *p*-R'ArCO$_2$H in the homoleptic series of (a) [Ru$_2$(*p*-R'ArCO$_2$H)$_4$(THF)$_2$] and (b) the heteroleptic series of [Ru$_2$(*p*-R'ArCO$_2$H)$_2${2,6-(CF$_3$)$_2$ArCO$_2$}$_2$(THF)$_2$], where the red and blue dots represent ***p*-CHO** and **Hete-*p*-CHO**, respectively. **1** (orange), **2** (light blue), **3** (pink), and **4** (light green). The dotted line represents the linear least-squares fit line. The black dots represent the corresponding homoleptic and *trans*-heteroleptic compounds, and the $E_{1/2}$ values were obtained from Ref. 17, 18, 19, 20, 21,22.

**References in SI**


1 R. W. Mitchell, A. Spencer, G. Wilkinson, *Dalton Trans.* 1973, 846–854.
2 F. A. Cotton, Y. Kim, A. Yokochi, *Inorg. Chim. Acta*, 1995, **236**, 55–61.
3 E.A. Boudreaux, L. N. Mulay, Theory and Applications of Molecular Paramagnetism. John Wiley & Sons, New York, 1976
4 CrysAlisPro ver. 1.171.41.89a, Rigaku Oxford Diffraction, 2020.
5 O. V. Dolomanov, L. J. Bourhis, R. J. Gildea, J. a. K. Howard, H. Puschmann, *J. Appl. Crystallogr.* 2009, **42**, 339–341.
6 G. Sheldrick, *Acta Crystallogr.* 2015, **71**, 3–8.
7 M. J. Frisch, G. W. Trucks, H. B. Schlegel, G. E. Scuseria, M. A. Robb, J. R. Cheeseman, G. Scalmani, V. Barone, B. Mennucci, G. A. Petersson, H. Nakatsuji, M. Caricato, X. Li, H. P. Hratchian, A. F. Izmaylov, J. Bloino, G. Zheng, J. L. Sonnenberg, M. Hada, M. Ehara, K. Toyota, R. Fukuda, J. Hasegawa, M. Ishida, T. Nakajima, Y. Honda, O. Kitao, H. Nakai, T. Vreven, J. A. Montgomery Jr., J. E. Peralta, F. Ogliaro, M. Bearpark, J. J. Heyd, E. Brothers, K. N. Kudin, V. N. Staroverov, R. Kobayashi, J. Normand, K. Raghavachari, A. Rendell, J. C. Burant, S. S. Iyengar, J. Tomasi, M. Cossi, N. Rega, J. M. Millam, M. Klene, J. E. Knox, J. B. Cross, V. Bakken, C. Adamo, J. Jaramillo, R. Gomperts, R. E. Stratmann, O. Yazyev, A. J. Austin, R. Cammi, C. Pomelli, J. W. Ochterski, R. L. Martin, K. Morokuma, V. G. Zakrzewski, G. A. Voth, P. Salvador, J. J. Dannenberg, S. Dapprich, A. D. Daniels, Ö. Farkas, J. B. Foresman, J. V. Ortiz, J. Cioslowski, D. J. Fox, Gaussian 09, Revision B.01, Gaussian, Inc., Wallingford CT, 2009.
8 A. D. Becke, *J. Chem. Phys*. 1993, **98**, 5648–5652.
9 P. J. Hay, W. R. Wadt, *J. Chem. Phys*. 1985, **82**, 299–310.
10 L. E. Roy, P. J. Hay, R. L. Martin, *J. Chem. Theory Comput*. 2008, **4**, 1029–1031.
11 A. W. Ehlers, M. Böhme, S. Dapprich, A. Gobbi, A. Höllwarth, V. Jonas, K. F. Köhler, R. Stegmann, A. Veldkamp, G. Frenking, *Chem. Phys. Lett*. 1993, **208**, 111–114.
12 P. C. Hariharan, J. A. Pople, *Theor. Chim. Acta* 1973, **28**, 213–222.
13 M. M. Francl, W. J. Petro, W. J. Hehre, J. S. Binkley, M. S. Gordon, D. J. DeFrees, J. A. Pople, *J. Chem. Phys*. 1982, **77**, 3654–3665.
14 T. Clark, J. Chandrasekhar, P. V. R. Schleyer, *J. Comput. Chem*. 1983, **4**, 294–301.
15 R. Krishnam, J. S. Binkley, R. Seeger, J. A. Pople, *J. Chem. Phys*. 1980, **72**, 650–654.
16 P. M. W. Gill, B. G. Johnson, J. A. Pople, M. J. Frisch, *Chem. Phys. Lett*. 1992, **197**, 499–505.
17 H. Miyasaka, N. Motokawa, R. Atsuumi, H. Kamo, Y. Asai, M. Yamashita, *Dalton Trans*, 2011, **40**, 673-682.
18 W. Kosaka, M. Itoh and H. Miyasaka, *Dalton Trans*., 2015, **44**, 8156–8168.
19 Y. Sekine, K. H. Aliyah, T. Shimada, J. Zhang, W. Kosaka and H. Miyasaka, *Chem. Lett*., 2018, **47**, 693–696.
20 W. Kosaka, Y. Watanabe, K. Aliyah, H. Miyasaka, *Dalton Trans*. 2022, **51**, 85–94.
21 W. Kosaka, Y. Watanabe, C. Itoh and H. Miyasaka, *Chem. Lett*., 2022, **51**, 731–734.
22 M. H. Chisholm, G. Christou, K. Folting, J. C. Huffman, C. A. James, J. A. Samuels, J. L. Wesemann and W. H. Woodruff, *Inorg. Chem*., 1996, **35**, 3643–3658.